Quantized Motion of Cold Cesium Atoms in Two- and Three-Dimensional Optical Potentials

G. Grynberg,[1] B. Lounis,[2] P. Verkerk,[1] J.-Y. Courtois,[1] and C. Salomon[2]

[1]*Laboratoire de Spectroscopie Hertzienne de l'Ecole Normale Supérieure, Université Pierre et Marie Curie, Case 74, T 12-E 01, F-75252 Paris CEDEX 05, France*

[2]*Laboratoire de Spectroscopie Hertzienne, Département de Physique de l'Ecole Normale Supérieure, 24 rue Lhomond, F-75231 Paris CEDEX 05, France*

(Received 23 November 1992)

Quantization of atomic motion is observed in two- and three-dimensional cesium optical molasses by stimulated Raman spectroscopy. A new geometry is used with the minimum number of laser beams, so that the topography of the optical potential is not sensitive to phase drifts of the molasses beams. The deepest potential wells are located on hexagonal lattice in two dimensions and on a body-centered-cubic lattice in three dimensions. They correspond to purely circularly polarized light, allowing a Lamb-Dicke narrowing of the transitions between vibrational levels to occur.

PACS numbers: 32.80.Pj

Despite the rapid progress in the understanding of cold atoms [1], their behavior in three-dimensional standing waves (optical molasses) is still far from being completely understood. For example, the analogy between an optical molasses and a viscous fluid is often used [2]. In such a description, atoms appear as classical particles subjected to a damping force and to heating mechanisms due to the atom-field interaction. Many experiments involving temperature measurements or velocity damping [3] are satisfactorily described by these models. By contrast, such a description becomes questionable when accounting for localization of atoms to less than an optical wavelength in a three-dimensional (3D) molasses [4]. Moreover, recent experiments in a one-dimensional (1D) molasses have shown that a significant fraction of the atoms undergo a quantized oscillatory motion around their equilibrium position [5,6]; in addition, these experiments demonstrated that a long-range spatial order, similar to that found in crystals, but with a spatial period of the order of the optical wavelength, can occur [5,7]. A fundamental question is that of whether these new quantum systems might also be observed in higher dimensions. On the theoretical side, the extension of the band model from 1D [8] to 2D [9] is very computationally demanding. On the experimental side, it was shown in [5] that the most convenient condition for observing quantization of the atomic motion is to have a geometry for the molasses beams for which the polarization of light is purely circular at the points where the atoms experience the largest light shift: The Lamb-Dicke narrowing of the Raman transitions [10] then allows a clear separation of the vibrational lines. A possible 2D geometry is to use two linearly cross-polarized standing waves propagating in orthogonal directions. Quantization of the atomic motion has actually been observed very recently in this situation [11]. However, such a scheme requires a locking of the phase difference between the two standing waves to a particular value. Any significant shift or drift of this phase modifies the topography of the optical potential associated with the light shifts and leads to a disappearance of the vibration spectrum [11]. We present here new 2D and 3D geometries for the molasses beams where the shape of the optical potential is not sensitive to any phase drift of the molasses beams. A phase shift just induces a global translation of the optical potential which keeps the same topography. With these beam configurations, quantized atomic motion in the potential wells induced by the molasses beams is easily observed in both 2D and 3D.

Consider a molasses created by p beams in an n-dimensional space ($p > n$). The atom-field interaction induces an optical potential due to the light shifts which depends on the relative phases of the incident beams. The number of independent relative phases being $p-1$ and the number of independent space translations being n, phase drifts are equivalent to space translations as long as $p=n+1$. Hence, a phase shift induces a global translation of the optical potential in which the atomic dynamics are unaffected as long as the phase changes remain slow on the scale of the typical atomic evolution time. To take advantage of this, one should use three beams in 2D experiments and four beams in 3D situations. Furthermore, one should look for the optical potential whose depth is maximum at points where the light polarization is purely circular, so that the lifetimes of the atoms in these wells are considerably lengthened by the very small drain to other levels [10].

The optical potentials for our molasses geometries are as follows [12]. In the 2D configuration, three coplanar beams of equal intensity, each separated by 120° [Fig. 1(a)] and linearly polarized in the plane of the beams, create a total field whose local polarization varies with space and which is perfectly circular for points located on an hexagonal lattice [Fig. 1(b)]. The light shifts being maximum at these points, one expects the atoms to be localized on this hexagonal pattern. This pattern, with its alternated σ^+ and σ^- potential wells, should lead to Sisyphus cooling [13] and to an antiferromagnetic order for the localized atoms [5]. In the 3D configuration [Fig. 2(a)], four beams travel along the threefold symmetry axes of a regular tetrahedron [14]. Three of the beams

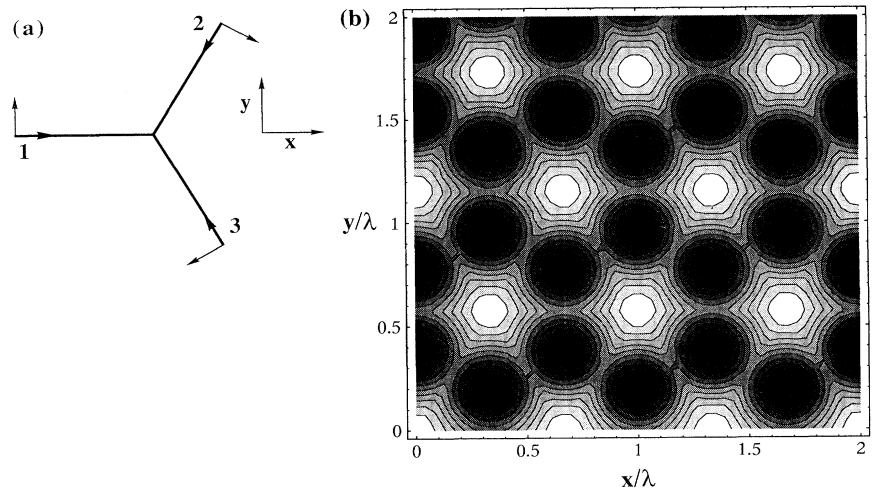

FIG. 1. Beam configuration for the 2D molasses. (a) Three coplanar beams of equal intensity have wave vectors making a 120° angle with each other. The three beams are linearly polarized in the plane of the figure. (b) Spatial dependence of the minima of the optical potential. The scale on both the x and y axes is the laser wavelength λ. The potential wells have their minima (which appear in black) on a hexagonal lattice, at points where the light polarization is purely circular.

have a linear polarization in a plane orthogonal to the propagation direction of beam 4, which is circularly polarized. The projection of this geometry onto a plane orthogonal to beam 4 looks similar to the situation of Fig. 1(a), but the addition of beam 4 breaks the symmetry between the σ^+ and σ^- potential wells. For a beam 4 σ^+ polarized, the potential wells associated with the σ^+ polarization are deeper than for σ^-, and hence the atoms are expected to be localized mainly in the σ^+ wells, which are located on a body-centered-cubic lattice [Fig. 2(b)]. Because the localized atoms have the same magnetization, this situation presents some analogy with a ferromagnetic medium [15].

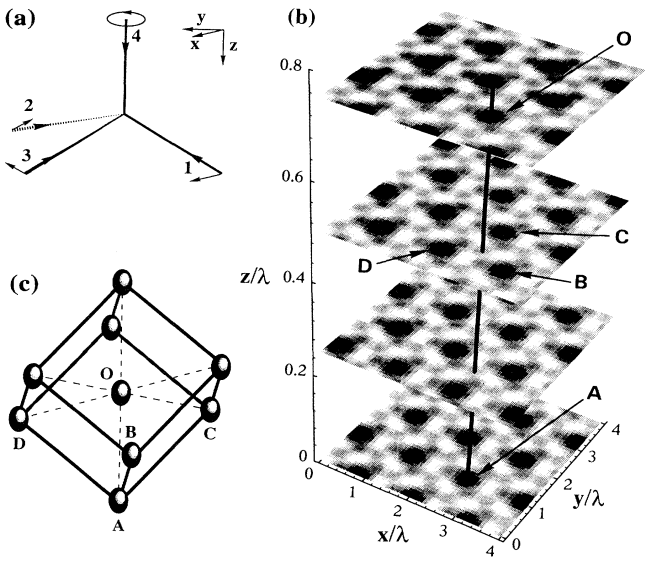

FIG. 2. Beam configuration for the 3D molasses. (a) Four beams travel along the threefold symmetry axes of a regular tetrahedron. Three equal intensity beams (1,2,3) have a linear polarization in the plane orthogonal to the propagation direction of beam 4, which is circularly polarized. (b) Minima of the optical potential (represented by the darkest zones). The potential wells have their minima on a body-centered-cubic lattice, at points where the light is σ^+ polarized. The four planes shown in the figure are perpendicular to the propagation direction of beam 4, which is a diagonal of the cubic unit cell shown in (c). The periodicity of the optical potential along the z axis is equal to $3\lambda/4$.

We first describe the experiments performed with a 2D geometry. The principle of the probe transmission experiments is described in our earlier paper [5]: Cesium atoms are cooled and trapped in a cell magneto-optical trap [16]. After some time, both the trapping beams and the inhomogeneous magnetic field are switched off, and three molasses beams, each having an intensity $I=5$ mW/cm^2, and a probe beam of intensity $I_p=0.1$ mW/cm^2 are sent through the cloud of cold cesium atoms [Fig. 3(a)]. The transmitted probe intensity is recorded versus the frequency difference $\omega_p-\omega$ between probe and molasses beams [Fig. 3(b)]. Stimulated Raman resonances between quantized vibrational states having a width (≈ 25 kHz FWHM) much smaller than the optical pumping rate are observed. This shows that the actual lifetimes of the lowest vibrational levels are considerably lengthened in the Lamb-Dicke regime [5,10], as expected for this 2D geometry [17]. The positions of the Raman resonances of Fig. 3(b) are in good agreement with the values of the oscillation frequencies predicted from the variation of the light shifts near the bottom of the optical potential wells. In particular, we checked that the positions of the Raman lines were independent of the probe direction (the bottom of the potential wells can be described by an harmonic potential having a cylindrical symmetry), and that they varied at low saturation at $\sqrt{I/|\Delta|}$ in agreement with theory (the detuning from resonance Δ was varied from -3Γ to -16Γ where Γ is the excited state linewidth). The asymmetry between stimulated absorption and emission in Fig. 3(b) is due to the

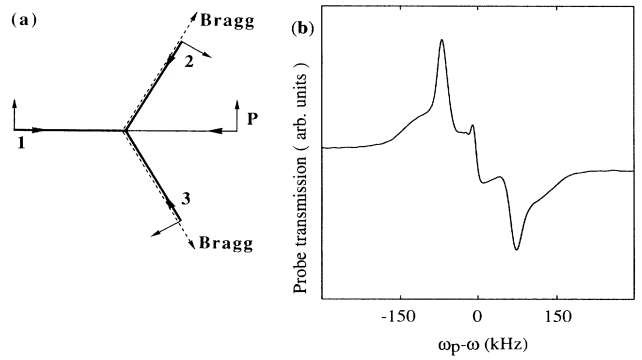

FIG. 3. Beam configuration for the 2D experiments. (a) The probe beam P propagates in the direction opposite to beam 1. (b) Probe transmission vs $\omega_p-\omega$ for a detuning $\Delta=-10\Gamma$. Very narrow Raman resonances corresponding to transitions between vibrational levels in the potential wells are symmetrically located around ω. The difference between absorption and amplification is due to the fact that propagation is nonlinear because of the optical thickness of the molasses.

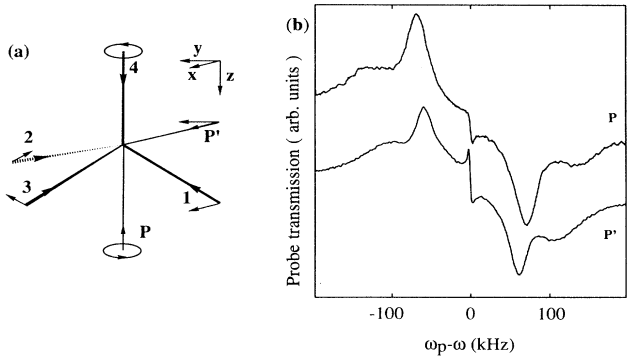

FIG. 4. Beam configuration for the 3D experiments. (a) Two weak beams propagate in directions opposite (P) and orthogonal (P') to beam 4 (P' is polarized along y). (b) Simultaneous recording of probe transmissions vs $\omega_p-\omega$ for beams P and P'. The detuning is $\Delta=-12\Gamma$. The oscillation frequencies are different because of the nonsphericity of the optical potential near its minima. Note that overtones are clearly visible.

large amplification and absorption experienced by the probe beam during propagation (Raman gains as large as 70% were measured). Stimulated Rayleigh resonances were also observed on probe transmission spectra [Fig. 3(b)]. Extending the results of [10], one can infer that these narrow resonances are associated with the long decay times of the populations in the bound vibrational levels, and that they are sensitive to the atomic localization and spatial order.

We now describe the experiments performed with the 3D geometry of Fig. 2(a). The experiment is performed in the same way as for the 2D case, i.e., by applying the four molasses beams (having diameters ≈ 0.8 cm and intensities $I\approx 4$ mW/cm^2) when the magneto-optical trap is switched off. However, because the cooling is now three dimensional, the molasses lifetime is much longer (≈ 1 s instead of 10 ms in the 2D case) [18]. For the geometry of Fig. 2(a), the bottoms of the potential wells are expected to have an ellipsoidal rather than a spherical symmetry because of the polarization asymmetry between beam 4 and the other beams. We thus used two weak beams to probe independently the directions both parallel and orthogonal to beam 4 [Fig. 4(a)]. We show in Fig. 4(b) the corresponding probe transmission spectra versus $\omega_p-\omega$. Narrow Raman resonances are observed in both spectra, but their positions differ, indicating the occurrence of two different vibrational modes with different oscillation frequencies. Furthermore, when we decrease the intensity of beam 4, we observe that the oscillation frequency along Oz decreases more rapidly than the oscillation frequency in xOy, as expected from theory. A particularly interesting result concerns the very steep Rayleigh resonances (having a peak to peak distance of the order of 2 kHz), which demonstrate the occurrence of very long decay times for the populations of the vibrational levels.

We wish now to comment on the possibility to prove the crystalline arrangement of atoms using Bragg scattering of light. It is well known in solid-state physics that the Bragg diffraction of an incident beam of wave vector $\mathbf{k}_p$ only occurs in directions $\mathbf{k}_s$ for which $\mathbf{k}_s=\mathbf{k}_p+\mathbf{K}$ (where $\mathbf{K}$ is a vector of the reciprocal lattice), provided that $k_s=k_p$ [19]. For the lattices displayed in Figs. 1(b) and 2(b), a simple calculation shows that $\mathbf{k}_i-\mathbf{k}_{i+1}$ are basis vectors of the reciprocal lattice ($\mathbf{k}_i$ is the wave vector of the molasses beam i). For example, in the 2D experiment, and for the probe direction of Fig. 3(a), Bragg diffraction is thus expected in the directions $\mathbf{k}_p+\mathbf{k}_1-\mathbf{k}_2$ and $\mathbf{k}_p+\mathbf{k}_1-\mathbf{k}_3$. When $\mathbf{k}_p\approx-\mathbf{k}_1$, Bragg scattering occurs in directions nearly opposite to the propagation direction of the molasses beams $\mathbf{k}_2$ and $\mathbf{k}_3$. We actually observed for nearly degenerate probe and cooling beams a strong emission in both directions, the intensity of each diffracted beam being on the order of 2% of the probe intensity. In normal crystals, the difference in momentum between the incident and the diffracted beams is absorbed by the lattice. In the present situation, because atoms are bound by the molasses beams, momentum conservation implies that the change of momentum of the scattered photon should be compensated for by photon redistribution in the molasses beams. This is why the vectors of the reciprocal lattice are linear combinations of $\mathbf{k}_i-\mathbf{k}_j$. It can also be noted that this Bragg condition is nothing but the phase-matching condition for a four-wave mixing process. Such an interpretation is consistent with the preceding analysis, because emission due to four-wave mixing occurs in the directions for which the atomic momentum is unchanged [20]. The observation of Bragg diffraction of light is thus not a proof of crystal order.

In conclusion, we observed quantized atomic motion in

2D and 3D optical molasses. The occurrence of a Lamb-Dicke narrowing of the vibrational lines demonstrates that atoms are localized near points where light is purely circularly polarized, and the measured vibrational frequencies are in agreement with theoretical predictions made for the potential wells of Fig. 1(b) and 2(b). Although we have no *direct* access to the molasses lattice structure, we can infer from the preceding results that atoms are localized in potential wells belonging to a hexagonal lattice in the 2D experiment, and to a body-centered-cubic lattice in the 3D configuration.

We believe that the laser beam geometries presented in this paper will prove interesting for future experiments. For example, in the 3D lattice, we reached densities where at most one site in ten was occupied by a cold atom. There is still a large majority of unoccupied sites, and hence the probability of having two atoms in the same potential well is consequently small. Quantum statistical effects which are not important for the results presented here could thus become noticeable with an increase of 1 order of magnitude in the density. The ease with which such a density can be achieved is not yet clear, but the goal does not seem unrealistic and appears to be a fascinating challenge for future research.

We would like to thank C. Cohen-Tannoudji, K. Berg-Sørensen, Y. Castin, and J. Dalibard for helpful discussions. Laboratoire de Spectroscopie Hertzienne is a unité de recherche de l'Ecole Normale Supérieure et de l'Université Pierre et Marie Curie, associé au CNRS. This work has been supported by DRET (No. 89214) and CNES (No. 910414).

[1] See, for instance, the special issue on laser cooling and trapping of atoms, edited by S. Chu and C. Wieman [J. Opt. Soc. Am. B **6** (1989)]; C. Cohen-Tannoudji and W. D. Phillips, Phys. Today, No. 10, 33 (1990).

[2] S. Chu *et al.*, Phys. Rev. Lett. **55**, 48 (1985).

[3] P. Lett *et al.*, Phys. Rev. Lett. **61**, 169 (1988); D. S. Weiss *et al.*, J. Opt. Soc. Am. B **6**, 2072 (1989); C. Salomon *et al.*, Europhys. Lett. **12**, 683 (1990); B. Lounis *et al.*, Phys. Rev. Lett. **69**, 3029 (1992).

[4] C. I. Westbrook *et al.*, Phys. Rev. Lett. **65**, 33 (1990); N. P. Bigelow and M. G. Prentiss, Phys. Rev. Lett. **65**, 30 (1990).

[5] P. Verkerk *et al.*, Phys. Rev. Lett. **68**, 3861 (1992).

[6] P. S. Jessen *et al.*, Phys. Rev. Lett. **69**, 49 (1992).

[7] B. Lounis *et al.*, Europhys. Lett. **21**, 13 (1993).

[8] Y. Castin and J. Dalibard, Europhys. Lett. **14**, 761 (1991).

[9] K. Berg-Sørensen *et al.* (to be published).

[10] J.-Y. Courtois and G. Grynberg, Phys. Rev. A **46**, 7060 (1992).

[11] A. Hemmerich and T. W. Hänsch, Phys. Rev. Lett. **70**, 410 (1993). We thank the authors for having communicated a preprint of their results.

[12] In general, the force experienced by cold atoms can be split into two parts: one associated with the optical potential and one accounting for radiation pressure effects [C. Cohen-Tannoudji, in *Fundamental Systems in Quantum Optics,* Proceedings of the Les Houches Summer School, Session LIII, edited by J. Dalibard, J. M. Raimond, and J. Zinn-Justin (Elsevier Science, Amsterdam, 1991). Contrary to the 1D lin $\perp$ lin geometry, the radiation pressures exerted by the cooling beams do not cancel at each point in the 2D and 3D molasses presented here. Near the bottom of the optical potential wells where quantization of atomic motion is probed, the restoring force associated with the optical potential overcomes the resultant radiation pressure by a factor of the order of $|\Delta|/\Gamma$ (the ratio of the detuning from resonance to the linewidth of the excited state), so that in first approximation the atom-field interaction can be described in terms of the optical potential only, when $|\Delta|/\Gamma \gg 1$. Such a condition (which is required anyhow to observe quantization of atomic motion) is fulfilled in our experimental conditions where $|\Delta|/\Gamma \approx 10$.

[13] J. Dalibard and C. Cohen-Tannoudji, J. Opt. Soc. Am. B **6**, 2023 (1989).

[14] Note that a magneto-optical trap using circularly polarized beams in a tetrahedral configuration was previously reported by F. Shimizu *et al.*, Opt. Lett. **16**, 339 (1991).

[15] We used another 3D geometry where beam 4 is linearly polarized. This case also corresponds to a body-centered-cubic lattice but the basis now consists of two potential wells (one for each circular polarization). For this situation, which leads to experimental spectra similar to the one presented in Fig. 4, the medium is antiferromagnetic.

[16] C. Monroe *et al.*, Phys. Rev. Lett. **65**, 1571 (1990).

[17] By contrast, when the linear polarization of one of the molasses beams is $\pi/2$ rotated, the narrow Raman resonances disappear, because the polarization of light is no longer circular at the positions where the light shifts are maximum.

[18] As mentioned in [12], the radiation pressures exerted by the cooling beams do not cancel at each point in the molasses. In particular, one might suspect the atoms to be efficiently expelled from the molasses along wires where the total electric field exhibits a purely traveling component, due to the destructive interference between beams 1, 2, and 3 [see Fig. 2(a)]. However, the occurrence of very long trapping times demonstrates that it is not the case. One can actually show that because of interference processes between the contributions of the four cooling beams the resulting force is not aligned along the wires, and thus prevents the atoms from escaping the trap.

[19] C. Kittel, *Introduction to Solid State Physics* (Wiley, New York, 1962).

[20] C. Cohen-Tannoudji, J. Dupont-Roc, and G. Grynberg, *Atom-Photon Interactions* (Wiley-Interscience, New York, 1992), p. 105.

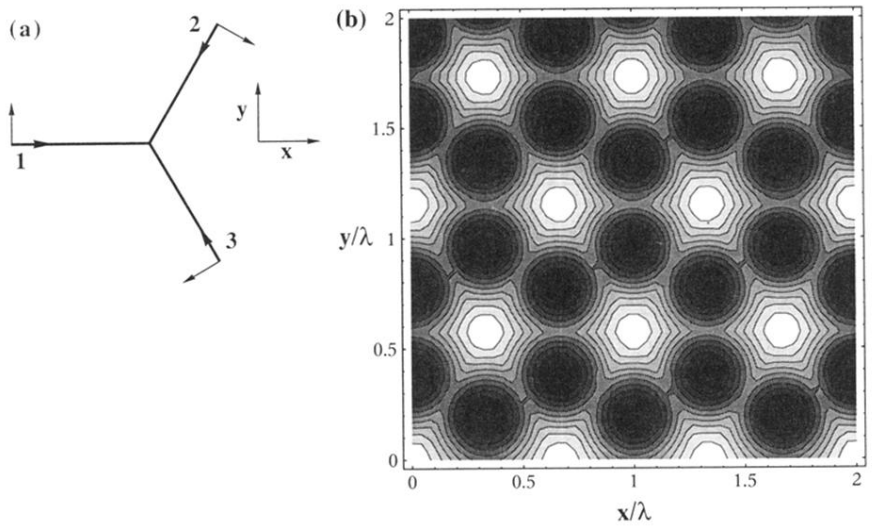

FIG. 1. Beam configuration for the 2D molasses. (a) Three coplanar beams of equal intensity have wave vectors making a 120° angle with each other. The three beams are linearly polarized in the plane of the figure. (b) Spatial dependence of the minima of the optical potential. The scale on both the x and y axes is the laser wavelength λ. The potential wells have their minima (which appear in black) on a hexagonal lattice, at points where the light polarization is purely circular.

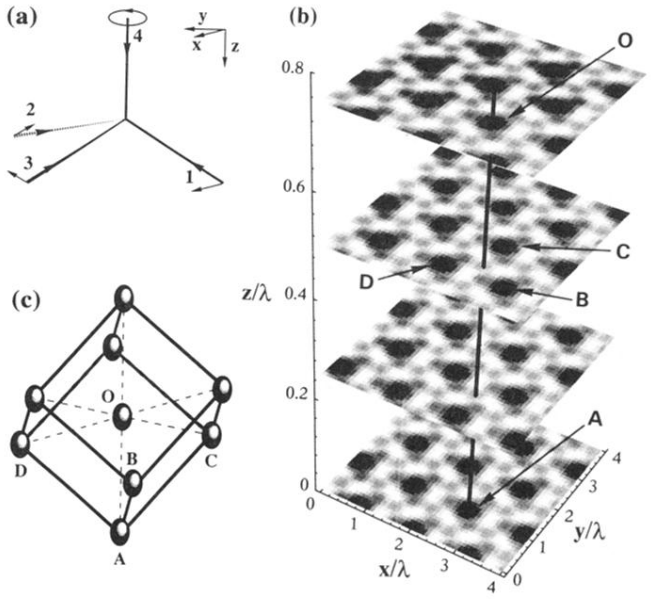

FIG. 2. Beam configuration for the 3D molasses. (a) Four beams travel along the threefold symmetry axes of a regular tetrahedron. Three equal intensity beams (1,2,3) have a linear polarization in the plane orthogonal to the propagation direction of beam 4, which is circularly polarized. (b) Minima of the optical potential (represented by the darkest zones). The potential wells have their minima on a body-centered-cubic lattice, at points where the light is σ^+ polarized. The four planes shown in the figure are perpendicular to the propagation direction of beam 4, which is a diagonal of the cubic unit cell shown in (c). The periodicity of the optical potential along the z axis is equal to $3\lambda/4$.